Harmful Interference Threshold and Energy Detector for On-Board Interference Detection

Christos Politis Sina Maleki Symeon Chatzinotas Björn Ottersten
SnT-Interdisciplinary Centre for Security, Reliability and Trust, University of Luxembourg
4, rue Alphonse Weicker, L-2721 Luxembourg
e-mail:{christos.politis, sina.maleki, symeon.chatzinotas, bjorn.ottersten}@uni.lu

***Abstract*—Interference issues have been identified as a threat for satellite communication systems and services, resulting in throughput degradation and revenue loss to the satellite operators. The situation is likely to become worse over the next years, as new services are deployed. In this context, an on-board spectrum monitoring unit (SMU) is proposed to detect interference reliably. Current satellite SMUs are deployed on the ground and the introduction of an in-orbit SMU can bring several benefits, e.g. simplifying the ground based station in multi-beam systems. Furthermore, the interference to signal plus noise ratio (ISNR) threshold on the uplink of a satellite forward link is identified as the harmful interference threshold above which the SMU needs to reliably detect interference. Moreover, this paper introduces the hypothesis testing problem required for the detection of interference and provides a performance analysis of the energy detector (ED) to solve this problem. Finally, simulation results are provided for validation.**

I. Introduction

Interference is the undesired power contribution of other carriers in the frequency band occupied by the desired carrier [1], and has been identified as a major threat for satellite communication systems and services [2]. Interference has a financial impact on the satellite operators that can run into several million dollars [3]. The situation is likely to become worse over the next years, as new services are deployed.

Interference on satellite communications (SATCOM) can be classified into two categories: internal or intra-system interference, and external interference. The internal and external interference is produced over carriers transmitted from Earth stations belonging to the same and different systems, respectively. Both of these categories of interference can be further characterized as narrowband or wideband interference [4]-[5]. Some potential sources of internal interference in the satellite network are: co-channel interference, adjacent channel interference and cross-pol interference [6]-[7]. Some examples of potential external interference sources are: adjacent system interference, in-line interference and intentional interference [6], [8]. Furthermore, according to ITU Radio Regulations [9], all these types of interference are categorized as permissible, accepted and harmful interference. Harmful interference is highly undesirable in a communication system.

Effectively tackling interferences is a complex task to be performed at various levels: interference monitoring; interference detection and isolation; interference classification; interference localisation; and interference mitigation. In this paper, we focus on the detection of interference. A method to detect interference is the use of a spectrum monitoring unit. While current satellite SMUs are deployed on the ground [10]-[11], there are some attempts to design in-orbit tools for this purpose [12]. The introduction of an in-orbit SMU would bring several benefits, e.g. allowing faster reaction to resolve interference before the downlink impairment; simplifying the ground based stations in multi-beam satellites by avoiding equipment replication in multiple Earth stations; and simplifying the separation between interference and signal, as the noise contribution is low. However, the on-board implementation faces some technical challenges, which have to be taken into account, with the most important to be the minimization of the complexity/power consumption.

In this paper, we develop the required algorithm to calculate the minimum detectable interference (i.e., the harmful interference threshold). This algorithm can be used in order to calibrate the on-board interference detection module. Although the underlaying algorithms are developed for the static scenarios, they can be easily extended to the dynamic cases when the dynamic channel variations in the uplink and downlink of the satellite are available. We further introduce the so called hypothesis testing problem required for detection of interference and provide a performance analysis of a simple detector namely energy detector [13]-[17] to solve this problem. The ED problem has a plethora of applications, however, to the best of our knowledge, application of the ED for interference detection is not considered before, especially for low ISNR. Note that this work should be seen as the starting point towards a unified framework for future activities, defining the requirements of on-board SMUs, as well as more complicated techniques which need to be developed for weak interference detection.

The remainder of this paper is organized as follows. In Section II, the system description and signal model is provided. The harmful interference analysis is presented in Section III. The ED is discussed in Section IV. Numerical results are depicted in Section V. Finally, Section VI concludes the paper and discusses about the future work.

II. Signal model and system description

As mentioned in Section I, there are several benefits of carrying out interference detection on-board the satellite. To reap these benefits, one possible solution is to include, within the payload, a dedicated on-board SMU. The knowledge of harmful interference threshold could help the SMU to

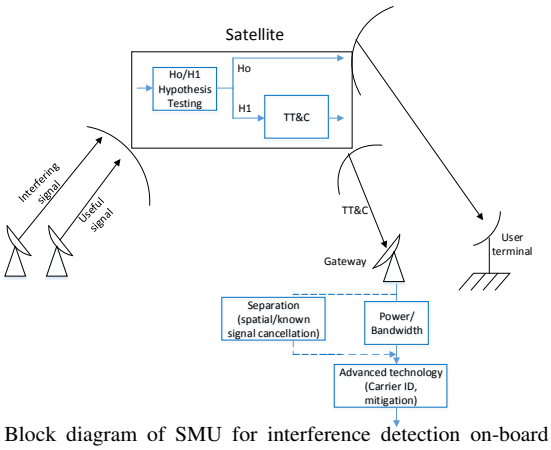

Fig. 1: Block diagram of SMU for interference detection on-board the satellite.

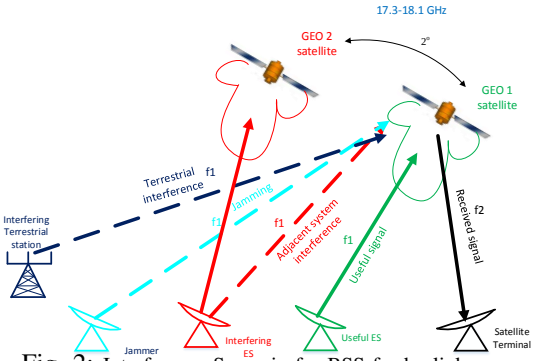

Fig. 2: Interference Scenario for BSS feeder link.

implement and calibrate a number of detection algorithms to identify any interfering carriers. Figure 1 depicts a simple block diagram of the SMU for interference detection on-board a satellite equipped with simple digital transparent processor (DTP). We consider a scenario where a single antenna is employed by the satellite to detect interference, while the transmitter and the interferer have only one transmit antenna. The detection problem can be formulated as the following binary hypothesis test:

$$H_0 \quad : x(n)=s(n)+w(n), \qquad n = 0, ..., N-1 \quad (1)$$

$$H_1 \quad : x(n)=s(n)+w(n)+i(n), \quad n = 0, ..., N-1 \quad (2)$$

where $w(n)$ is the additive noise at the receiving satellite antenna, modelled as an independent and identically distributed (i.i.d.) complex Gaussian vector with zero mean and variance σ^2, $s(n)$ is the primary signal at the receiving satellite antenna and $i(n)$ is the interfering signal at the receiving satellite antenna to be detected. In SATCOM literature [18]-[20], we can see that under clear sky conditions, the satellite feeder link channel is assumed ideal and in that case, the $s(n)$ and $i(n)$ are assumed to be a complex Gaussian random vector, with zero mean and covariance R_s and R_i, respectively. However, when the satellite feeder link operates in a frequency above 10 GHz, then it is subjected to various atmospheric fading effects, degrading the performance of the system [21]. The most important factor is the rain attenuation.

If the hypothesis H_1 is validated, this information is reported to the ground through the telemetry, tracking and command (TT&C), otherwise if the hypothesis H_0 is confirmed, there is no need for action, and the signal follows the downlink transmission. Then, advanced signal processing algorithms (beam-forming, Carrier ID [22], ...) take place in the on-ground processing unit. In the next section, we identify the minimum ISNR which needs to be detected by the SMU.

III. Harmful Interference

In Figure 2, an interference scenario, imposed by several sources on the broadcasting satellite services (BSS) feeder link, in Ka-band 17.3-18.1 GHz is considered. Our goal is the calculation of the minimum detectable interference on the uplink, under clear sky and rainy conditions for this scenario. Based on some link budget equations (the analytical methodology is presented in Appendix A), the minimum detectable interference on the uplink, I_U, is derived

$$I_U \leq \frac{EIRP_{ES} G_{RSL,max}}{\gamma L_U} - N_U - \frac{EIRP_{ES} G_{RSL,max} L_D N_D}{EIRP_{SL} G_{Re,max} L_U} \ (W). \quad (3)$$

where, $EIRP_{ES}$ and $EIRP_{SL}$ are the effective isotropic radiated power (EIRP) at the Earth station and satellite, respectively, $G_{RSL,max}$ and $G_{Re,max}$ are the maximum gain of the receiving antenna of the satellite and the ground station, respectively, L_U and L_D are the losses on the uplink and downlink, respectively, N_U and N_D are the noise power on the uplink and downlink, respectively, γ is the value of SINR in the user terminal and finally I_U is the aggregated power received by the receiving antenna of the satellite, transmitted by the interfering stations. Furthermore, the indices U and D represent the uplink and downlink, respectively.

IV. Energy Detector

As shall be shown in Section V, the contribution of noise in our interference scenario is negligible and hence, we can simplify our hypothesis test of (1), (2) as follows:

$$H_0 \quad : x(n)=s(n), \qquad n = 0, ..., N-1 \quad (4)$$

$$H_1 \quad : x(n)=s(n)+i(n), \quad n = 0, ..., N-1 \quad (5)$$

For this new hypothesis testing, if the covariance R_s and R_i of the desired and interfering signal are both known, the Neyman-Pearson approach [12] leads to the estimator-correlator detector that is optimal for the hypothesis testing problem in (4) and (5). However, in the case that $R_s = \sigma_s^2$ and $R_i = \sigma_i^2$ we can prove that the ED of (6) is the optimal. This is a good assumption in the sense that time dispersion is almost non-existent in satellites, particularly in the fixed satellite services (FSS) geostationary (GEO) satellites.

$$T(\mathbf{x}) = \sum_{n=0}^{N-1} x^2[n] > \epsilon \quad (6)$$

where ϵ is the selected threshold in order to decide the presence or absence of the interference.

In this paper, we study the ED only under clear sky conditions (AWGN case). The study of the ED for rainy conditions, which entails integration over possible channel variations, is considered for future studies. The two important parameters in order to determine the performance of the energy detector are the probability of false alarm (P_{FA}) and the probability of detection (P_D), where $P_{FA} = Q_{x^2_{2N}}\left(\frac{\epsilon}{\sigma_s^2}\right)$ and $P_D = Q_{x^2_{2N}}\left(\frac{\epsilon}{\sigma_s^2+\sigma_i^2}\right)$, follow a chi-square χ^2 distribution [13] with $2N$ degrees of freedom, where N is the number of samples. Furthermore, according to [23] the asymptotic performance of the ED, can be approximated by (7) and (8), respectively

$$P_{FA} = Q\left(\left(\frac{\epsilon}{\sigma_s^2} - 1\right)\sqrt{N}\right) \tag{7}$$

$$P_D = Q\left(\left(\frac{\epsilon}{(\gamma+1)\,\sigma_s^2} - 1\right)\sqrt{N}\right) \tag{8}$$

The main design parameters of the energy detector are the threshold and the number of samples. The threshold based on the P_{FA}, in order to detect interference, is given

$$\epsilon = \left(\frac{Q^{-1}\left(P_{FA}\right)}{\sqrt{N}} + 1\right)\sigma_s^2 \tag{9}$$

Furthermore, for a given pair of target probabilities (P_{FA}, P_D), the number of required samples to achieve these targets can be determined from (7) and (8) by cancelling out the threshold variable ϵ [14]. The result is given by $N = \left(\frac{Q^{-1}(P_{FA})-(\gamma+1)Q^{-1}(P_D)}{\gamma}\right)^2$.

Finally, if we look at (9), we notice that the threshold selection depends on the signal power. Therefore, the accurate knowledge of the signal power at the receiver is required. If there is signal power uncertainty, then, the number of samples is given according to [24] by $N = \left(\frac{Q^{-1}(P_{FA})-(\gamma+1)Q^{-1}(P_D)}{\gamma-\left(\eta-\frac{1}{\eta}\right)}\right)^2$, where the signal uncertainty factor can be defined as $B = 10\log_{10}\eta$ [25]-[26].

V. Numerical results

A. Harmful Interference

In the following graphs, we see how the link budget affects the interference threshold in our BSS scenario, considering the long-term fading models instead of the short-term ones. The BSS feeder links are located in Betzdorf, Luxembourg and we consider a carrier frequency of 17.7 GHz. In our numerical results, the GEO terminals are located in the edge of the beam (considering a worst-case broadcasting scenario) of the GEO satellite (ASTRA 4A of SES), located in 23.5° East, specifically in Thurso, Scotland and we assume a carrier frequency of 19.7 GHz. The link budget parameters for the Ka band GEO satellite are presented in Table 1 [27].

Figure 3 depicts the link based interference threshold versus the signal to interference plus noise ratio (SINR) in the terminal, for clear sky and rainy conditions. We assume that the range of SINR is from -2.4 to 16.1 dB (values for the lowest and highest modulation and coding (ModCod) in DVB-S2 standard [28]). For the rainy conditions, the rainfall rate on the uplink and downlink is fixed, 30 mm/h and 25 mm/h, respectively, which represents the chance of 0.01% during the whole year. In this figure, as expected, we can see that the interference tolerance threshold increases as the SINR reduces. Furthermore, we can notice that there is a SINR wall, above which the satellite terminals cannot be delivered with the requested data rates. Moreover, this figure presents the ISR or ISNR above which interference considered as harmful for a specific SINR. Finally, we notice that the values of ISR range from 3 to -16 dB under clear sky conditions and 3 to -24 dB under rainy conditions, which means that we have to develop algorithms, which work properly for low ISRs.

TABLE I: LINK BUDGET PARAMETERS FOR A KA-BAND GEO SATELLITE

Parameter	Value
Parameters for satellite	
orbit	GEO circular
Satellite height	35786 km
Satellite noise temperature	575 K
Satellite EIRP	72 dBW
Polarization	Single
Elevation angle	30.74^o
Max. antenna Rx gain	42 dBi
Feeder loss in the receiver	1 dB
Polarization loss	1 dB
Depointing loss	1 dB
Parameters for gateway	
Uplink carrier frequency	17.7 GHz
Gateway location	49.68^o N, 6.35^o E
Gateway EIRP	80 dBW
Uplink free space loss	208.47 dB
Atm. Atten. (clear sky)	0.3 dB
Parameters for user terminal	
Downlink carrier frequency	19.7 GHz
Receiver location	58.59^o N, 3.5^o W
Terminal antenna diameter	0.75 m
Terminal antenna efficiency	60 %
Elevation angle	19.5^o
Downlink free space loss	209.4 dB
Sky noise temperature	20 K
Ground noise temperature	10 K
Feeder loss in the receiver	1 dB
Polarization loss	1 dB
Depointing loss	1 dB

Figure 4 extends the work more and shows the signal to noise ratio (SNR), the ISNR, the ISR and the interference to noise ratio (INR) threshold on the uplink versus the SINR in the terminal, for the clear sky and rainy conditions, respectively. From this graph, we can notice that the level of interference is much higher than the level of noise, especially for low SINRs, therefore the contribution of the noise is negligible and hence, as we mentioned earlier, we can simplify our hypothesis testing problem of (1), (2) in this of (4), (5).

B. Energy Detector

Here, we present simulation results to illustrate the detection performance of the proposed interference detection technique. Throughout this section, we assume that the transmitter, the interferer and the receiver (satellite) have only one antenna. We assume that the transmitted useful and interfering signals are

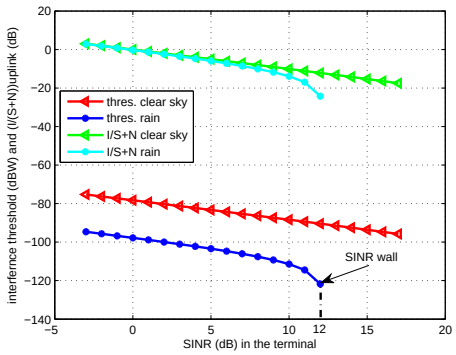

Fig. 3: Interference tolerance threshold and ISNR on the uplink versus the SINR (uplink: Betzdorf, elevation angle=30.74°, f=17.7 GHz, $R_{0.01}$=30 mm/h, downlink: Thurso, elevation angle=19.7°, f=19.7 GHz, $R_{0.01}$=25 mm/h).

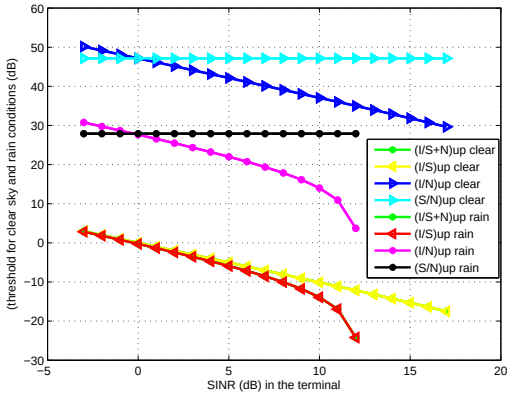

Fig. 4: comparison of different interference threshold versus the SINR under clear sky and rain conditions (uplink: Betzdorf, elevation angle=30.74°, f=17.7 GHz, $R_{0.01}$=30 mm/h, downlink: Thurso, elevation angle=19.7°, f=19.7 GHz, $R_{0.01}$=25 mm/h).

i.i.d complex Gaussian random variables. 10,000 Monte Carlo simulations are carried out with each simulation consisting of $N = 250$ independent observation samples. Furthermore, we assume 0.5 dB signal uncertainty, denoted as ED (0.5dB). The ISR ranges from -25 to 5 dB, which the values of ISR that we are interested in, as we showed earlier.

Figure 5 shows the probability of interference detection versus the ISR for different probabilities of false alarm. We can notice that when the P_{FA} increases, the P_D increases. Furthermore, Figure 5 presents the probability of interference detection versus the ISR for a fixed $P_{FA} = 0.1$, comparing the ED with and without signal uncertainty. If the signal variance is unknown, even with only 0.5dB signal uncertainty, the ED performs much worse than the ideal ED, which knows the signal variance.

Finally, Figure 6 depicts the required number of samples that we need in order to detect interference for a fixed $P_D = 0.99$ and $P_{FA} = 0.1$. Also, we can see how the sample complexity N varies for the energy detector as the ISR approaches the ISR wall, where the ISR wall reflects the fact that the energy detector cannot robustly detect interference, if the interference

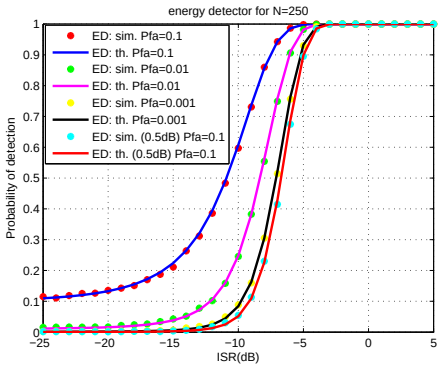

Fig. 5: P_D versus the ISR for different values of P_{FA}.

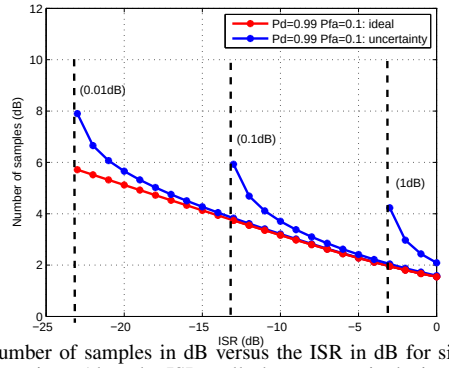

Fig. 6: Number of samples in dB versus the ISR in dB for signal with and without uncertainty. Also, the ISR wall phenomenon is depicted.

power is less than the uncertainty in the signal power [24].

VI. Conclusion

In this paper, we discussed the phenomenon of interference on the uplink of a BSS feeder link in Ka-band. A formula was derived in order to define harmful interference threshold for on-board interference detection module. Moreover, we showed that the contribution of noise on the uplink is negligible, hence the binary hypothesis test of (1), (2) can be simplified, ignoring the noise. Finally, we presented the detection performance of the energy detector, noticing that firstly requires a large number of samples for the detection of low ISRs and secondly that results in the ISR wall, in the case that we do not have accurate knowledge of the signal power at the receiver. Hence, in the future work more sophisticated interference detection algorithms will be examined, in order to tackle the weak interference detection scenarios. Furthermore, another issue would be to realistically model the spectral properties of the DVB signals instead of assuming Gaussians.

Appendix

In this appendix, the derivation of (3) is shown in details.

A. Clear sky conditions

The total SINR of the system is given by [1]

$$\left(\frac{S}{I+N}\right)_T^{-1} = \left(\frac{S}{N}\right)_U^{-1} + \left(\frac{S}{N}\right)_D^{-1} + \left(\frac{S}{I}\right)_U^{-1} + \left(\frac{S}{I}\right)_D^{-1}, \quad (10)$$

where $\left(\frac{S}{N}\right)_U$ and $\left(\frac{S}{I}\right)_U$ are the uplink SNR, and the uplink signal to interference ratio (SIR) at the satellite receiver input, respectively, and $\left(\frac{S}{N}\right)_D$ and $\left(\frac{S}{I}\right)_D$ are the downlink SNR, and the downlink SIR at the terminal station, respectively. In this paper, we assume that there is no interference in the downlink. As far the other factors of (10), we can obtain them as follows,

$$\left(\frac{S}{N}\right)_U = \frac{EIRP_{ES} G_{RSL,max}}{L_U N_U}, \tag{11}$$

$$\left(\frac{S}{N}\right)_D = \frac{EIRP_{SL} G_{Re,max}}{L_D N_D}, \tag{12}$$

$$\left(\frac{S}{I}\right)_U = \frac{EIRP_{ES} G_{RSL,max}}{L_U I_U}, \tag{13}$$

The losses, for the uplink and downlink, are classified into the following types: L_{FS} is the free space loss, L_A is the attenuation of waves and it is affected only by the gases in the atmosphere. L_{FRX} and L_R is the feeder and depointing losses in the receiving equipment, respectively and L_{POL} is the polarization mismatch loss. Therefore, $L_U = L_{FS,U} L_{A,U} L_{R,U} L_{FRX,U} L_{POL,U}$ and $L_D = L_{FS,D} L_{A,D} L_{R,D} L_{FRX,D} L_{POL,D}$.

The N_U is given by the Nyquist equation as follows, $N = kTB\ (W)$, where k is the Boltzmann constant $1.38 \times 10^{-23}\, JK^{-1}$, T is the system noise temperature and B is the bandwidth of the wanted modulated carrier. The system noise temperature consists of the noise from: the antenna, T_A, feeder losses, T_F, and receiver, T_R. Therefore, T is obtained by [1] $T = \frac{T_A}{L_{FRX}} + T_f\left(1 - \frac{1}{L_{FRX}}\right) + T_R\ (K)$. The antenna noise temperature on the downlink, $T_{A,D}$, is defined as the contribution of the clear sky noise plus the noise from the ground as $T_{A,D} = T_{SKY} + T_{GROUND}\ (K)$.

SINR should have a threshold γ that offers sufficient quality of service (QoS). Inserting (11), (12) and (13) in (10), we obtain

$$SINR = \frac{A}{B + C} \geq \gamma, \tag{14}$$

where: $A = EIRP_{ES} EIRP_{SL} G_{RSL,max} G_{Re,max}$, $B = EIRP_{SL} G_{Re,max} L_U (N_U + I_U)$ and $C = EIRP_{ES} G_{RSL,max} L_D N_D$.

Based on (14), the minimum detectable interference on the uplink I_U is derived and shown in (3).

B. Rainy conditions

A similar formula as in (3) is used in the rainy scenario. However, now $L_A = A_{GAS} + A_{RAIN}\ (dB)$ and $T_{A,D} = \frac{T_{SKY}}{A_{RAIN}} + T_m(1 - A_{RAIN}) + T_{GROUND}\ (K)$, where T_m is the mean thermodynamic temperature.

Finally, the value of attenuation due to A_{RAIN} is given by the product of the specific attenuation γ_R (dB/km) and the effective path length of the wave in the rain L_e (km), as follows [1], [29] $A_{RAIN} = \gamma_R L_e\ (dB)$.

ACKNOWLEDGEMENT

This work was supported by the National Research Fund, Luxembourg under the CORE project SATSENT: Satellite Sensor Networks for spectrum monitoring and SEMIGOD: Spectrum Management and Interference Mitigation in Cognitive Radio Satellite Networks.

REFERENCES

[1] G. Maral and M. Bousquet, *Satellite Communication Systems*, Wiley, 2009.

[2] ESA ARTES 5.1 Statement of Work, "On board spectrum monitoring".

[3] R. Ames, "Satellite interference: What it means for your bottom life," www.integ.com/is3/whitepapers/sktelecommnews.pdf.

[4] J.A. Lzaro, "GNSS Aray-based Acquisition: Theory and Implementation," PhD dissertation, Centre Technolgic de Telecommunications de Catalunya, July 2012.

[5] Rec. ITU-R S.741-2, "Carriers-to-interference calculations between networks in the fixed satellite service," Geneva, 1994.

[6] L. Castanet, A. Bolea-Alamanac and M. Bousquet, "Interference and fade mitigation techniques for Ka and Q/V band satellite communication systems," *in Proc. Int. Workshop on COST Actions 272 and 280*, Noordwijk, The Netherlands, May 2003.

[7] R. Rideout, "Technologies to identify and/or mitigate harmful interference," *in International satellite communication workshop on the ITU- challenges in the 21st century: Preventing harmful interference to satellite systems*, June, 2013.

[8] A. Vallet, "Harmful interference to satellite systems," *in International satellite communication workshop*, Geneva, 2013.

[9] ITU, "Radio Regulations," Geneva, 2012.

[10] SIEMENS, "SIECAMS®," http://www.convergence-creators.siemens.com/bundles/cms/downloads/2214-BSIECAMS-R01.0-EN.pdf.

[11] SAT CORPORATION, "Monics®," http://www.sat.com/~/media/sat/literature/monics%20brochure.pdf.

[12] QINETIQ, "Frequency Monitoring Payload," http://www.qinetiq.com/services-products/space/Pages/satellite-payloads-fmp.aspx.

[13] S. M. Kay, *Fundamentals of Statistical Signal Processing: Detection Theory*, Upper Saddle River, NJ: Prentice-Hall, 1998.

[14] H. Urkowitz, "Energy detection of unknown deterministic signals,"*Proc. of the IEEE*, vol. 55, no. 4, pp. 523 531, April 1967.

[15] F. Digham, M.-S. Alouini, and M. Simon, "On the energy detection of unknown signals over fading channels,"*in IEEE Int. Conf. Commun.*, vol. 5, may 2003, pp. 3575 3579.

[16] F. Digham, M.-S. Alouini, and M.K. Simon, "On the energy detection of unknown signals over fading channels,"*IEEE Trans. Commun.*, vol. 55, no. 1, pp. 21 24, jan. 2007.

[17] S. Atapattu, C. Tellambura, and H. Jiang, "Performance of an energy detector over channels with both multipath fading and shadowing,"*IEEE Trans. Wireless Commun.*, vol. 9, no. 12, pp. 3662 3670, december 2010.

[18] B. Devillers, A. Perez-Neira, and C. Mosquera,"Joint linear precoding and beamforming for the forward link of multi-beam broadband satellite systems," *in IEEE Global Telecommunications Conference (GLOBECOM)*, Houston, Texas, USA, Dec. 2011.

[19] D. Christopoulos, S. Chatzinotas, G. Zheng, J. Grotz, and B. Ottersten, "Linear and nonlinear techniques for multibeam joint processing in satellite communications," *EURASIP journal on wireless communications and networking*, vol. 2012, pp. 113, May 2012.

[20] J. Arnau, B. Devillers, C. Mosquera, and A. Perez-Neira, "Performance study of multiuser interference mitigation schemes for hybrid broadband multibeam satellite architectures," *EURASIP Journal on Wireless Communications and Networking*, vol. 2012, pp. 119, Apr. 2012.

[21] A. D. Panagopoulos, P.-D. M. Arapoglou, and P. G. Cottis, "Satellite communications at Ku, Ka and V bands: propagation impairments and mitigation techniques," *IEEE Commun. Surveys & Tutorials*, vol. 6, no. 3, pp. 214, third quarter, 2004.

[22] M. Coleman, "Fighting Interference with technology," *in* 30^{th} *Space Symposium, Technical Track*, Coloralo, May 2014.

[23] Y.-C. Liang, Y. Zeng, E. Peh, and A. T. Hoang, "Sensing-Throughput Tradeoff for Cognitive Radio Networks,"*in ICC proceedings*, 2007.

[24] R. Tandra, A. Sahai, "SNR Walls for Signal Detection,"*IEEE journal of selected topics in signal processing*, vol. 2, no. 1, February 2008.

[25] R. Zhang, T. J. Lim, Y.-C. Liang, and Y. Zeng, "Multi-Antenna Based Spectrum Sensing for Cognitive Radios: A GLRT Approach,"*IEEE transactions on communications*, vol. 58, no. 1, January 2010.

[26] Pu Wang, J. Fang, N. Han, and H. Li, "Multiantenna-Assisted Spectrum Sensing for Cognitive Radio,"*IEEE transactions on vehicular technology*, vol. 59, no. 4, May 2010.

[27] S.K. Sharma, S. Chatzinotas and B. Ottersten, "Inline Interference Mitigation Techniques for Spectral Coexistence of GEO and NGEO Satellites," *International Journal of Satellite Communications and Networking*, 2014.

[28] ROHDE&SCHWARZ, "Second Generation DVB via Satellite: DVB-S2", Training Center Munich, Germany, 2009.

[29] Rec. ITU-R P.618-11, "Propagation data and prediction methods required for the design of Earth-space telecommunication systems," Geneva, 2013.